
Surface freezing of chain molecules at the liquid–liquid and liquid–air interfaces

Eli Sloutskin,^a Colin D. Bain,^b Benjamin M. Ocko^c and Moshe Deutsch*^a

^a *Physics Department, Bar-Ilan University, Ramat-Gan 52900, Israel. E-mail: deutsch@mail.biu.ac.il; Fax: +972 (0)3 5353298; Tel: +972 (0)3 5318476*

^b *Department of Chemistry, Oxford University, Mansfield Rd., Oxford, UK OX1 3TA*

^c *Physics Department, Brookhaven National Laboratory, Upton NY 11973, USA*

Received 21st April 2004, Accepted 9th July 2004

Surface freezing (SF) is the formation of a crystalline monolayer at the free surface of a melt at a temperature T_s , a few degrees *above* the bulk freezing temperature, T_b . This effect, *i.e.* $T_s > T_b$, common to many chain molecules, is in a marked contrast with the surface melting effect, *i.e.* $T_s \leq T_b$, shown by almost all other materials. Depending on chain length, n , the SF layer shows a variety of phases, in some cases tuneable by bulk additives. The SF behaviour of binary mixtures of different-length alkanes and alcohols is governed by the relative chain length mismatch, $|\Delta n/n|^2$, yielding a quasi-“universal” behaviour for the freezing of both bulk and surface. While SF at the liquid–air interface was studied rather extensively, Lei and Bain (*Phys. Rev. Lett.*, 2004, **94**, 176103) have shown only very recently that interfacial freezing (IF) can be induced also at the water : tetradecane interface by adding the ionic surfactant CTAB to the water phase. We present measurements of the interfacial tension of the water : hexadecane interface, as a function of temperature and the ionic surfactant STAB, revealing IF at a STAB-concentration-dependent temperature $T_i > T_b$. The measurements indicate that a single frozen monolayer is formed, with a temperature-existence range of up to 10 °C, much larger than the 1.2 °C found for SF at the free surface of the melt. We also find a new effect, where the IF allows tuning of the interfacial tension between the two bulk phases to zero for a range of temperatures, $\delta T = T_{\text{mix}} - T_b \leq T_i - T_b$ by *cooling* the system below T_i . We discuss qualitatively the factors stabilizing the frozen layer and their variation from the liquid–air to the liquid–liquid interfaces. The surfactant concentration dependence of T_i is also discussed and a tentative theoretical explanation is suggested.

Introduction

The phase behaviour of matter is, in general, a function of the dimensionality. Thus, the phase sequences of thin films and surfaces were expected,¹ and found experimentally,² to differ from those of the three-dimensional bulk. In particular, for melting of a solid both theory and experiment show that with very few exceptions it is the *less ordered surface* which coexists with the *more ordered bulk*, *i.e.* the quasi-2D surface melts at a temperature lower than, or, at most, equal to that of the 3D bulk. This phenomenon, called surface melting, has been found for almost all solids studied to date.² This is easy to understand, since a molecule at the surface is less restricted, and hence has a higher entropy, than a molecule residing deep in the bulk. A much less common, and less understood,

phenomenon is surface freezing, where an *ordered surface layer* coexists with a *disordered bulk* liquid. No experimental observation of this effect at a free surface was reported, to the best of our knowledge, for any material prior to 1992, when the first measurements revealed the SF effect in melts of normal alkanes ($\text{CH}_3(\text{CH}_2)_n - \text{CH}_3$, hereafter denoted C_n).³ A somewhat related effect of a smectic surface layer coexisting with a less-ordered nematic or isotropic bulk, has been observed previously in liquid crystals.⁴ However, the surface layer did not show any lateral *crystalline*-like order, as did the SF layer of alkane melts.

Since this paper focuses on the alkane–water interface, only the SF behaviour of alkanes will be discussed in some detail below.⁵ However, it should be noted that numerous chain molecules (*e.g.* alcohols, semi-fluorinated alkanes, alkyl-thiols, α,β -diols, alkyl-oligoethyleneglycols, 1-alkenes, *etc.*), though not all, also exhibit SF.⁶ Fatty acids and other normal-alkane derivatives with bulky headgroups, and chain molecules with non-linear tails, do not seem to undergo SF. The structure of the SF layer varies considerably from one molecule to another, and depends also on the existence of additional intermolecular interactions. For example, for 1-alcohols,⁷ where hydrogen bonding exists between the hydroxyl headgroups, SF yields a crystalline bilayer, rather than the monolayer found in alkanes. This, in turn, allows for the intercalation of either water,⁸ or diols⁹ into the center of the bilayer, inducing new phases and structures.

Several theoretical explanations have been proposed for the occurrence of SF in chain molecules. The experimental results strongly point to the chain-like structure of the molecule as the major cause for surface freezing. One approach argues that the lower density of the CH_3 end groups imparts them a slightly higher surface activity. The surface enrichment of the end groups induces a preferential vertical alignment of the alkane chains even at $T > T_s$, leading eventually to a more ordered phase at the surface.¹⁰ Density functional theories for molecules with weak anisotropy also yield a preferential surface-normal molecular alignment at the liquid surface, inducing, in turn, the SF effect.¹¹ Molecular simulations with various models also find SF for chain molecules, and investigate its length dependence.¹² Tkachenko and Rabin¹³ suggested an entropic stabilization. Since the molecules are long, large vertical thermal fluctuations, and hence a large entropy, are allowed without violating the Lindemann criterion for crystal melting. This entropy stabilizes the SF layer. This approach explains both the role of the chain structure in the occurrence of the surface freezing effect and the lower chain length limit for the occurrence of SF. Recently, conformational entropy due to chain-end disorder, argued to be higher at the surface than at the bulk, was also suggested as the stabilizing agent of the SF layer.¹⁴ While the question “what drives SF in chain molecules” is far from being settled, it should be noted that SF can be explained as a pure wetting effect, resulting from a particular balance of free energy excesses and deficits at the surface, without the need to resort to a molecular-level theory.^{5,15}

SF is not restricted to the liquid–vapour interface. It has been detected also in the freestanding thin films of bubble walls, where SF increases significantly the bubble’s lifetime and changes its coalescence behaviour.¹⁶ SF has also been detected and studied in thin alkane films at the solid–vapour interface,¹⁷ where it influences significantly the phase sequence measured, and the structures formed in the films with temperature variation.

SF at the liquid–liquid interface is much more elusive. For the *alcohol*–water interface, temperature-dependent surface tension measurements, $\gamma(T)$, reveal a sharp break in the curve a few degrees above the bulk freezing temperature of the alcohol. This break has been interpreted as either a transition from an expanded to a condensed interfacial phase,¹⁸ or as an interfacial crystallization transition.¹⁹ However, detailed X-ray and surface tension studies by Schlossman *et al.*²⁰ (see also contribution in this volume) on long-chain alkanol surfactants at the water : hexane interface indicate that the break observed in $\gamma(T)$ is in fact due to an adsorption transition from a low to a high density monolayer of alkanols at the interface. They also find that the alkanols’ chains, residing in the hexane, are progressively disordered with distance from the interface even in the low-temperature, high-density phase. An intercalation of water molecules into the alkanols’ headgroup layer, residing in the water phase, is also conjectured.

For the *alkane*–water interface, no SF was detected in spite of a rather extensive search at several laboratories. Considering that replacing the vapour phase by a water phase changes completely the energetics at the surface, and hence the balance allowing SF to occur at the liquid–air interface,¹⁵ this is not surprising. However, Lei and Bain²¹ have recently demonstrated that adding a small amount of the ionic surfactant CTAB to the water phase of a water : tetradecane system can re-shift

the balance, causing IF to emerge. We report here on surface tension measurements on this effect for a different system, water:hexadecane, with a different surfactant, STAB. The interfacial layer, which undergoes IF, consists of a binary mixture of two types of chains: the C18 tails of the STAB surfactant, adsorbed at the surface due to its amphiphilic nature, and the C16 molecules of the alkane phase. We will therefore discuss the present results within the context of the SF observed at the alkane-air interface, with particular reference to our recently-published theoretical and experimental study of SF at the free surface of melts of binary alkane mixtures.²²

Experimental

The details of the experiment, materials, and data analysis are available in refs. 5–9, 22–25 and will not be repeated here. The surface tension measurements employ the Wilhelmy plate method in a two-stage oven under computer control. The X-ray measurements described in the next section were carried out at beamline X22B, NSLS, Brookhaven National Laboratory, USA. The X-ray reflectivity (XR) and grazing-incidence diffraction (GID) measurements allow an Ångström-resolution determination of the SF layer's structure in the surface-normal, and the surface-parallel directions, respectively.

The air–melt interface

Pure alkanes. In spite of its relative simplicity, surface tensiometry is a sensitive tool for observing surface structure variations in layers as thin as a single monolayer. Fig. 1 shows a $\gamma(T)$ scan for the air–melt interface of C26. γ is the excess free energy at the surface over the bulk, $\gamma = \varepsilon_s - \varepsilon_b - T(S_s - S_b)$, where ε and S denote, respectively, the molecular energy and entropy and the subscripts s and b – the surface and bulk.²³ For simple liquids $S_s > S_b$ as discussed above, and hence, $d\gamma/dT = -(S_s - S_b) < 0$. An ordering of the surface, as occurs upon surface freezing, switches the slope to $d\gamma/dT > 0$, since now $S_s < S_b$. This is indeed observed in Fig. 1, where the abrupt slope change at T_s marks the SF transition, which is of first order, as expected from a freezing transition. The absence of additional slope changes for $T_b < T < T_s$ indicates that no other transitions occur in the surface-frozen layer from T_s down to T_b . The surface entropy change upon SF, ΔS , is derived from the slope change as $\Delta S = [d\gamma(T < T_s)/dT - d\gamma(T > T_s)/dT]$. The coincidence of this value, $\Delta S = 1.51 \text{ mN m}^{-1} \text{ K}^{-1}$, with the $1.52 \text{ mN m}^{-1} \text{ K}^{-1}$ calculated from the known *bulk* freezing entropy change for a single monolayer,⁵ indicates that the ordered surface layer is just one molecule thick. This conclusion is indeed supported by the X-ray measurements⁵ which probe directly the structure of the SF layer, and reveal a hexagonal packing with molecules aligned along the surface normal.

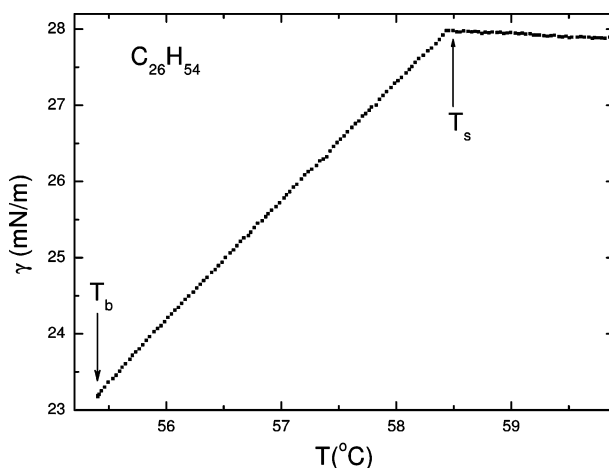


Fig. 1 Surface tension scan $\gamma(T)$ for C26 at the melt–air interface. T_b and T_s indicate the bulk and surface freezing temperatures. The change from a negative to positive slope upon decreasing T indicates an ordering transition at the surface.

The phase diagram in the (n, T) plane is shown in Fig. 2, along with additional quantities derived from the surface tension and X-ray measurements. As the figure indicates the SF layer exists only over a limited range in temperature and chain length. However, within this range several different phases are found. For $15 < n < 44$, the SF phase is a rotator, with vertically-aligned molecules up to $n < 30$, and tilted towards nearest neighbours by an n -dependent angle (5° for $n = 30$, 23° for $n = 44$) for $30 \leq n \leq 44$. For $n \geq 44$, the layer is a true herringbone-ordered crystal, with tilt in the next-nearest neighbour direction. The transitions with n between these phases are clearly observed, for example, in the changes they induce in ΔS in Fig. 2(b), where the slight slope decrease of the linear $\Delta S(n)$ marks the onset of the tilt at $n \approx 30$, and the large jump at $n = 44$ is due to a transition from a rotator to a crystalline surface phase. The measured layer thickness, D , and in-plane intermolecular distances, d , shown in Fig. 2(c,d), also reveal clearly the transition from untilted to tilted molecules, as well as the rotator-to-crystal transition. The known n -dependence of T_b , S_b , S_s and γ allows the derivation of a simple expression for the existence range, $\Delta T = T_s - T_b$, of SF: $\Delta T = a/n - b/n^3$. This functional form,²³ shown in a line in Fig. 2(a) accounts well for $\Delta T(n)$. Free-energy considerations,⁵ based on the balance among the various interfacial energies (SF layer/liquid bulk, SF layer/vapour, liquid surface/vapour) also allow accounting for the occurrence of SF, and for its n - and T -ranges of existence. The tilt and tilt-direction transition depend on more minor changes in the chain–chain interaction with n , and are more difficult to account for. The rotator-to-crystal transition in the SF layer as n is increased follows the same transition in the bulk for the first phase appearing upon freezing below the melt.

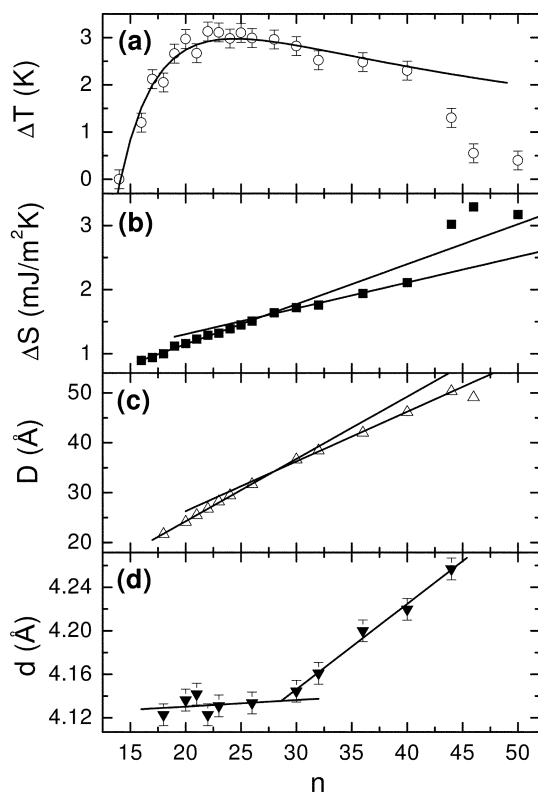


Fig. 2 (a) Length (n)—existence range ($\Delta T = T_s - T_b$) phase diagram (b) surface entropy change upon freezing (ΔS) (c) layer thickness (D) and in-plane nearest-neighbour spacing (d), for the surface-frozen layer of alkanes. Points denote measured values. Lines are guides to the eye, except in (a) where the theoretical line is discussed in the text.

Binary mixtures of alkanes. Binary mixtures of different-length alkanes also show SF. The variation of the fractional molar concentration ϕ of the longer component provides an additional “knob” allowing one to tune the SF effect to regions of phase space not reachable in pure materials. This results in the observations of new effects like a ϕ - or T -induced demixing transition in the solid surface layer manifested in an abrupt change in the thickness of the SF layer²⁴ and the only transition from a single to a double surface-frozen layer observed to date.²⁵

Fig. 3(a) and (c) show the measured ϕ -dependence of T_b and T_s for two typical mixtures, one with a small relative length mismatch, $\delta = \Delta n/\bar{n} = (n_1 - n_2)/[(n_1 + n_2)/2] \approx 0.095$, and one with a large one: $\delta \approx 0.33$. The two mixtures show a markedly different T_s and T_b behaviour. For small δ , the ϕ -variation is almost linear and monotonic, while for large δ the variation is more complex. The ϕ -variation of ΔS , the entropy change upon SF, derived from the slope change in the measured $\gamma(T)$ above and below T_s , is shown in Fig. 3(b) and (d). While the ϕ -variation of ΔS is continuous for small δ , it is clearly bimodal for large δ .

For the large- δ case, shown in Fig. 3(c,d), the two constant ΔS values, observed in the small ($0 \leq \phi \leq 0.18$) and large ($0.6 \leq \phi \leq 1$) ϕ -regions, equal those measured for the two pure components, C26 and C36, respectively. This indicates that a phase separation occurs at the surface in this case, and the SF layer of the mixture consists entirely of a single component: C26 at low ϕ and C36 at high ϕ . Indeed, X-ray measurements⁵ show a structure identical in each ϕ -region with that found for the SF layer of the melt of the corresponding pure component: an untilted rotator phase for C26, and a tilted rotator phase, with 18° tilt in the nearest-neighbour direction, for C36. As we show below, this phase separation is driven by the strong repulsion between the two species due to their large length mismatch, an effect well known for bulk polymer mixtures.²⁶ Note also the shaded region in Fig. 3(c), $0.18 \leq \phi \leq 0.4$, where no SF is observed, since it is preempted by bulk freezing, as observed in the coincidence of $T_s(\phi)$ and the $T_b(\phi)$ values in this range in Fig. 3(c). Also, in the range $0.4 \leq \phi \leq 0.5$, the exceptionally high ΔS values indicate the appearance of a different SF phase, having a smaller tilt, 13° , and a different tilt direction: towards the next-nearest neighbours.²⁷

For the small- δ case, shown in Fig. 3(a,b), the variation of ΔS with ϕ is continuous and monotonic. This indicates a mixed surface phase, where the mismatch interaction is too weak to induce phase separation. The X-ray results indeed show that the measured thickness of the SF layer coincides with that expected from ϕ assuming uniform mixing of the components.²²

These results, and similar ones measured for binary mixtures of alkanes spanning a broad range of δ , can be accounted for within the theory of mixtures, using the properties of the pure components and taking into consideration the mixing entropy and the molecular interactions.²⁶ In the liquid (l) state, where the molecules are flexible and space filling, we treat the bulk (b) and surface (s) phases as ideal mixtures, neglecting the very small mixing enthalpy expected. The free energy F_l^j per mole of a $C_n:C_m$ mixture is:²⁶

$$F_l^j = \phi_l^j f_l^j(n) + (1 - \phi_l^j) f_l^j(m) + kT_B [\phi_l^j \ln(\phi_l^j) + (1 - \phi_l^j) \ln(1 - \phi_l^j)] \quad (1)$$

where $j = s$ or b , $f_l^j = \varepsilon_l^j(i) - TS_l^j(i)$, $\varepsilon_l^j(i)$ and $S_l^j(i)$ are the molar free energy, energy and entropy, respectively, of pure C_i , $i = n$ or m , ϕ_l^j and $(1 - \phi_l^j)$ are the mole fractions of C_n and C_m , respectively. The term in the square brackets is due to the mixing entropy.²⁶ For the crystalline (c) phase, the chains are extended and aligned in parallel. The mismatch repulsion now entails a free energy cost of ω^j for interchanging a long and a short molecule.²⁷ The free energy is then:^{22,24,26}

$$F_c^j = \phi_c^j f_c^j(n) + (1 - \phi_c^j) f_c^j(m) + kT_B [\phi_c^j \ln(\phi_c^j) + (1 - \phi_c^j) \ln(1 - \phi_c^j)] + \omega^j \phi_c^j (1 - \phi_c^j) \quad (2)$$

where the notation of eqn. (1) is employed, with “crystalline” (c) replacing “liquid” (l). The last term in eqn. (2) is the repulsion term due to the interchange energy, ω^j , in the zeroth-order approximation (nearest neighbour interactions only) of the “strictly-regular” mixture theory.²⁶ The solid phase behaviour is now determined by the balance between the mixing entropy term and the interchange term. For $\omega^j \leq 2k_B T$ the mixing entropy dominates and a uniformly mixed crystalline phase is obtained at all ϕ_c^j . For $\omega^j \geq 2k_B T$, the repulsive term dominates and induces phase separation in the solid phase for compositions $\phi_c^j \approx 0.5$. Once phase separation occurs, eqn. (2), and the theory discussed here, cease to be valid, since for eqn. 2 a uniform mixing is required, with different-length molecules residing side by side. It is also important to note that the only quantity controllable experimentally is the bulk liquid composition, ϕ_l^b . All other quantities, e.g., the liquid

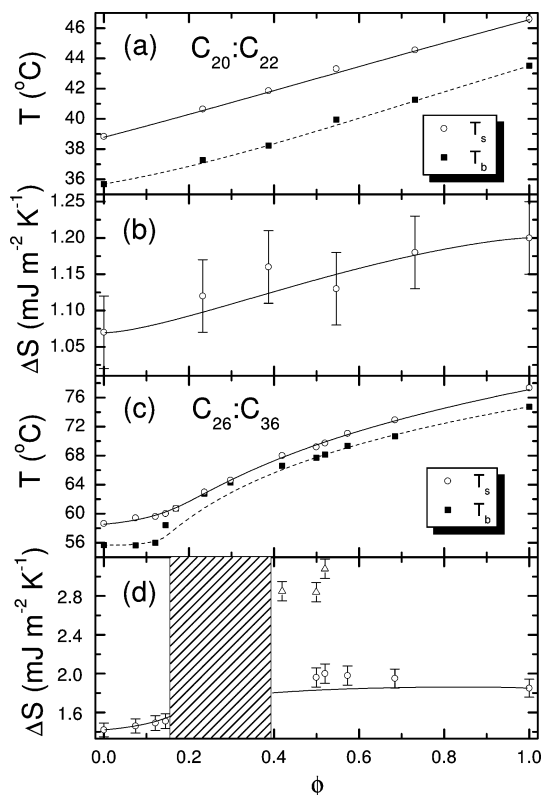


Fig. 3 (a,c) The measured (symbols) surface (T_s) and bulk (T_b) freezing temperatures for the mixtures indicated (b,d) the measured (symbols) surface entropy change upon freezing for the mixtures in (a) and (c). The lines in (a) and (c) are fits by the theory discussed in the text. This theory yields the lines shown in (b) and (d) without any adjustable parameters. The shadowed region in (d) indicates a fractional concentration (ϕ) range where surface freezing is not observed due to its pre-emption by bulk freezing.

and crystalline surface compositions, ϕ_1^s and ϕ_c^s , and the crystalline bulk composition, ϕ_c^b , are determined by the thermodynamics of the system. In particular, ϕ_1^s can be calculated from the known ϕ_1^b using the Gibbs adsorption rule, which yields, in our case, an enrichment of the surface by the shorter of the two components.

The chemical potentials calculated from eqns. (1) and (2) for the liquid and solid phases must be equal for each component at the freezing temperatures T_b and T_s . This yields equations for T_b and T_s in terms of the properties of the pure components (transition temperatures and entropy changes) appearing in eqns. (1) and (2), with ω^j as the only unknown parameter in each equation. For Cn :

$$T_j(\phi_1^j) = [T_{j,n}\Delta S_{j,n} - \omega^j(1 - \phi_c^j)^2]/[\Delta S_{j,n} + k_B \ln(\phi_c^j/\phi_1^j)] \quad (3)$$

where $T_{j,n}$ and $\Delta S_{j,n}$ are the known freezing temperature and the entropy change upon freezing of the pure component n . ω^j can now be obtained by fitting eqn. (3) to the measured $T_b(\phi_1^b)$ and $T_s(\phi_1^s)$ values, using a single ω^j (different for $j = b$ and $j = s$) for all concentrations ϕ_1^b of a given pair of alkane molecules. The equivalent expression for Cm , obtained by replacing $n \rightarrow m$ and $\phi_1^j \rightarrow (1 - \phi_1^j)$, is used to solve for ϕ_c^j numerically. The fits are shown in solid lines in Fig. 3(a,c), and clearly agree very well with the measured freezing temperatures in spite of the single fit parameter. Moreover, eqns. (1) and (2) allow also the calculation of $\Delta S(\phi_1^b)$, the concentration-dependent entropy change upon surface freezing of the mixture, without introducing additional parameters. This calculated $\Delta S(\phi_1^b)$ is shown as a solid line in Fig. 3(b,d). The good agreement, achieved without any adjustable parameters, further supports the validity of the analysis presented here.

An intriguing feature of the ω^j values derived for all the binary alkane mixtures studied is that they conform to a δ^2 dependence, $\omega^j = A\delta^2$, for both bulk and surface (albeit with a different prefactor A), as clearly demonstrated in Fig. 4. This is easy to rationalize as follows. The interchange energy ω^j should obviously depend on the chain length mismatch, Δn . However, a given mismatch Δn , which provides free volume for kinks, *gauche* conformations, *etc.*, should be relatively more important for a shorter molecule than for a longer one. It is therefore reasonable to assume that ω^j depends on $\delta = \Delta n/\bar{n}$, rather than on Δn only. Since $\delta < 1$ for all mixtures studied here, we can expand ω^j in a power series in δ , where the constant term vanishes, as identical molecules do not repel each other. Since only the absolute value of the mismatch counts, odd-power terms also vanish, leaving δ^2 as the lowest-order non-zero term. The series can be truncated after this term, since for $\delta \rightarrow 1$, where higher-order terms may be significant, phase separation of the components occurs anyway, and the theory above is not valid any more, as discussed above.²⁴

Fig 4 demonstrates that the ω^j values obtained from the measured data indeed conform exceedingly well to the expected linear δ^2 -dependence for ω^b up to $\delta^2 \approx 0.13$, which corresponds to $\omega^b \approx 2.5k_B T$, right at the limit of phase separation, which is also the limit of validity of our theory. For the surface, all mixtures studied, up to $\delta^2 \approx 0.23$, correspond to $\omega^s \leq 2.5k_B T$, and thus only the highest- δ^2 mixtures are close to phase separation. The higher prefactor A in the bulk (17.8 *vs.* 11.6) clearly indicates a higher inter-chain repulsion. This could possibly reflect larger strains in the crystal structure upon packing different chain lengths in a multilayered 3D solid, as compared to those in packing them in a single surface mono or bilayer.

A striking feature of the ω^j values of alkanes, and of those of binary mixtures of hydrated and dry alcohols, and deuterated-protonated alkanes (labeled D_n in Fig. 4),²² is the fact that all points fall on the *same* line, regardless of the components of the mixtures. This “quasi-universal” behaviour is surprising considering the presence of additional interactions in some of the mixtures: hydrogen bonding in alcohols and isotope mismatch repulsion in the deuterated-protonated alkane mixtures. While the isotope effect is expected to be small, hydrogen bonding is strong enough to induce the

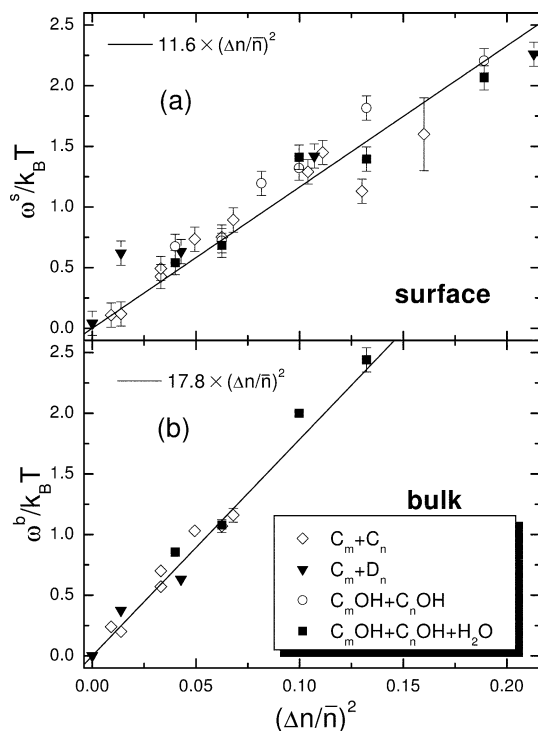


Fig. 4 The interchange parameter ω^j (symbols) derived from the theoretical fits shown in Fig. 3(a,c). Their quasi-“universal” linear dependence on the relative mismatch squared, δ^2 , is discussed in the text.

formation of a SF *bilayer* in alcohols, rather than the monolayer observed in alkanes. Moreover, hydration increases the strength of this interaction, as indicated by the higher transition temperatures measured for hydrated alcohol mixtures as compared to dry ones.⁸ Nevertheless, the “universal” behaviour found in Fig. 4 indicates that the length-mismatch repulsion energy of the chains dominate over any other interaction for the molecules studied.

Finally, we note that while the symmetry considerations above explain the observed δ^2 behaviour of the interchange energy ω^j , to the best of our knowledge, no theory predicting this behaviour from molecular-level considerations is available in the literature. The available molecular-level theories for polymer mixtures predict a $|\delta|$ dependence²⁸ or a $|\Delta n|$ dependence,²² both disagreeing with our measurements. A more sophisticated molecular-level theoretical treatment, taking into consideration the presence of voids, *gauche* kinks, short-range clustering of equal-length molecules, *etc.* may achieve a better agreement with experiment.

The water–melt interface

The temperature dependence of the interfacial tension. Measurements at several laboratories, including ours, failed to detect interfacial freezing (IF) at the alkane melt:water interface. This, however, is not surprising. The large-amplitude surface normal molecular vibrations invoked to provide entropic stabilization of the SF layer at the free surface of the melt¹³ may be greatly damped at an interface separating two dense liquid phases. A different proposed explanation for SF, a favourable balance between several surface tensions which drives the wetting of the free surface by a solid monolayer^{5,15} at $T_s > T_b$, is certain to unbalance when several of the surface tensions involved change drastically upon replacing the vapour phase with water. However, *in principle*, the free energy balance against the formation of an IF layer at the alkane melt–water interface could be returned to one favouring IF by adding a new, judiciously chosen interaction to the system. Lei and Bain²¹ demonstrated recently that this can be achieved by adding a cationic surfactant, cetyltrimethylammonium bromide (CTAB), at sub-mM concentrations, to the water phase of a water:C14 system. The resultant interfacial tension curves, $\gamma_i(T)$, are very similar to that in Fig. 1 where an abrupt slope change implies the occurrence of IF. They have also shown that the transition is not a CTAB adsorption/desorption transition of the type found by Schlossman *et al.*²⁰ for alcohols, since the surface excess of CTAB, derived from the variation of γ_i with concentration through the Gibbs rule, changes at the transition only insignificantly. These results, obtained at Oxford, have been subsequently verified at Bar-Ilan.

We have carried out interfacial tension measurements, using the Wilhelmy plate method in a two-stage computer controlled oven, on a different system, the water:C16 interface, using STAB (stearyl-trimethylammonium bromide) as a surfactant. The surfactant molecules adsorb at the interface, with their hydrophilic TAB headgroup residing in the water and their lipophilic stearyl (C18) tails protruding into the C16 phase. At the free surface of an alkane melt, sum frequency generation measurements indicate that the (fairly extended) chains align roughly along the surface-normal even in the liquid surface phase.²⁹ Similar measurements for CTAB at the water:C16 interface³⁰ show, however, that the interface-adsorbed CTAB chains are conformationally disordered. The chains adopt a more extended, upright conformation only when the saturation coverage is approached at the cmc. Fig. 5 shows measured interfacial $\gamma_i(T)$ curves in the absence and presence of STAB in the water phase. For pure water:C16 $\gamma_i(T)$ exhibits a constant negative slope down to T_b , as expected of a simple interface between two immiscible, mutually non-wetting, liquids. This indicates that no IF effect occurs at this interface, as found also for other water:C*n* interfaces.²⁰ When STAB is present, a slope change occurs in $\gamma_i(T)$ at a $T = T_i$ which depends on the STAB concentration, *c*. For $c = 0.133$ mM, a somewhat rounded slope-change occurs at $T_i \approx 24.3$ °C. For $c = 1.1$ mM a sharper slope change occurs at $T_i = 26$ °C. Both curves are very similar to that observed at the free surface of the melt, shown in Fig. 1, and to those reported for the water/C14/CTAB system.²¹ We assign, therefore, the break in $\gamma_i(T_i)$ here also to an IF transition. The slope changes yield an IF entropy change of $\Delta S^i = (0.86 \pm 0.05)$ and (0.78 ± 0.08) mJ m⁻² K⁻¹, for $c = 1.1$ mM and 0.133 mM, respectively, both close to the $\Delta S = 0.896$ mJ m⁻² K⁻¹ measured for the SF monolayer of C16 at the free surface.⁵ The coincidence between these ΔS values further supports the identification of the slope change as an IF effect, and suggests that the IF layer is a single monolayer thick. A point to note in Fig. 5 is that the Wilhelmy plate measuring the IF at the water:C16

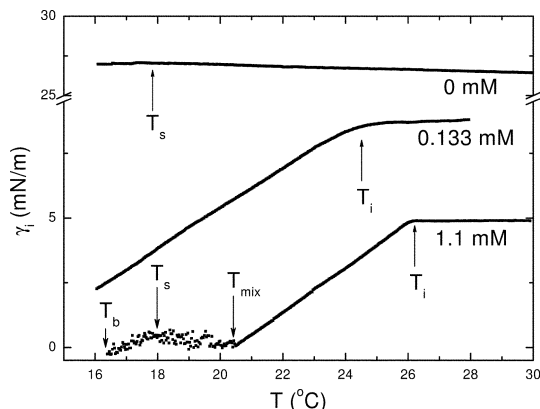


Fig. 5 The measured interfacial tension at the water:hexadecane interface without, and with the cationic surfactant STAB dissolved in the water phase at the indicated concentrations. Note, the abrupt slope change at T_i due to interfacial freezing, and the vanishing of the interfacial tension at T_{mix} for a STAB concentration of $c = 1.1$ mM. For discussion, see text.

interface is hanging from the film balance on a 0.6 mm diameter wire. This goes through the free surface of the C16, and thus senses the SF at the free surface, albeit as a very weak effect, due to the small diameter of the wire. This is observable in the $c = 0$ and $c = 1.1$ mM curves at $T_s \approx 17.8$ °C as a very small slope change.

The appearance of IF at the water: C_n interface raises some interesting possibilities concerning crystal nucleation of alkanes from the melt. One of the most widely used methods for achieving homogeneous nucleation from a melt is the dispersion of the melt into droplets in a carrier medium.³¹ If the melt can be divided finely enough, part of the droplets may be sufficiently pure and free from heterogeneous-nucleating agents to allow them to nucleate homogeneously. Alkanes-in-water emulsions, where the C_n droplets are stabilized by non-ionic surfactants, were shown to undergo homogeneous nucleation.³² However, the interfacial energetics in these droplets is radically different from that of a free surface of a melt, and IF is not expected, nor observed. This is manifested by the fact that an alkane melt having a free surface does not supercool, since SF produces a crystalline template already a few degrees above T_b , on which the bulk molecules can crystallize, and thus the barrier for crystal nucleation is eliminated. By contrast, a C_n emulsion's droplets, stabilized by non-ionic surfactants, *e.g.* Igepal, have been shown to undercool considerably, implying a nucleation barrier and no IF.³² However, using alkyl-TAB surfactants, rather than non-ionic ones, to stabilize the droplets should restore IF at the droplets' surface. This should, in principle, eliminate the supercooling in such emulsions. First calorimetry measurements indicate a reduction in the undercooling range of CTAB-stabilized C14 and C15 in water as compared to those stabilized by the non-ionic surfactant Igepal. The incomplete elimination of the nucleation barrier, indicated by the fact that undercooling does not vanish completely, is probably due to an imperfect matching between the structures of the IF layer and the critical nucleus, particularly since the latter may have a transient, non-equilibrium structure not matching that of a macroscopic crystal.³³

An even more intriguing possibility, provided by the formation of an IF layer, is the appearance of superheating. As pointed out by Frenkel³⁴ a solid with a free surface can not be superheated because surface melting invariably provides a liquid nucleus below the bulk melting point, which reduces to zero the nucleation barrier for the bulk liquid state. However, if surface freezing occurs, no liquid nucleus forms, and the non-zero nucleation barrier for the liquid state will allow one to superheat the bulk. A macroscopic-sized solid of alkane will always have heterogeneous nucleation sites like container walls, impurities, *etc.* Thus, even though SF will prevent formation of a liquid nucleus at the free surface upon heating past the equilibrium melting point, these sites will nucleate the melting. However, in C_n -in-water emulsions stabilized by alkyl-TAB surfactants, where IF occur over the full surface area of the (solid) emulsion particles, some particles may be free from liquid-nucleating agents. For those, IF will provide a kinetic barrier for melting, and thus allow

superheating. The barrier should yield a superheating range of up to the IF existence range, $\leq 10^\circ\text{C}$ in our case. A search for this effect is in progress.

The $\gamma_i(T)$ curve for $c = 1.1$ mM in Fig. 5 shows, in addition to IF, another interesting effect. The reduction of the surface tension of a liquid to zero by *heating* is common. It occurs, *e.g.*, at the liquid's critical point. Here we observed the opposite effect, the reduction of the interfacial tension to zero by *cooling*. This reduction of $\gamma_i(T)$ to zero is a new mechanism for the vanishing of the interfacial tension. It occurs here since below T_i we have $\gamma_i(T) = \gamma_i(T_i) - (T_i - T)(d\gamma_i/dT)$. Thus, $\gamma_i \rightarrow 0$ at $T_{\text{mix}} = T_i - \gamma_i(T_i)/(d\gamma_i/dT)$ unless preempted by bulk freezing of the alkane phase. At the free surface of a melt, and also at the solution : alkane interface at low surfactant concentrations, $\gamma_i(T_i)$ is usually large, and T_i is close to T_b , so that preemption indeed occurs, and vanishing of γ_i is not observed, as can be seen in the $c = 0.133$ mM curve in Fig. 5. The vanishing of γ_i can be induced in our system only because of the drastic reduction in γ_i from its high value at $c = 0$ to the much lower values obtained for large STAB concentrations. As observed in Fig. 5, for $c = 1.1$ mM γ_i vanishes at $T_{\text{mix}} = 20.4^\circ\text{C}$, 4.2°C above T_b . We find the same vanishing of γ_i for all curves measured at $c \geq 0.17$ mM. For $c \geq 0.2$ mM, we find a practically c -independent $T_{\text{mix}} = 20.4^\circ\text{C}$, resulting from the c -independent $T_i = 26^\circ\text{C}$ and $\gamma_i(T_i) \approx 5$ mN m $^{-1}$ for all $c \geq 0.2$ mM.

The ability to tune the interfacial tension γ_i to zero has several interesting implications. Usually, when γ_i between two separate phases vanishes, thermal diffusion will eventually lead to molecular-level mixing and form a uniform single phase. In our case, however, γ_i is zero only in the presence of the IF monolayer. Thus, the mixing can only occur by the formation of surfactant-coated C_n droplets. Thus, an emulsion is expected to form when the system is cooled below T_{mix} . However, in contrast with the usual emulsions, where the droplets are only metastable thermodynamically, and tend to coalesce with time, our “self-assembling” emulsion is stable under fluctuations, since $\gamma_i = 0$ and coalescence can not reduce the system's free energy. In our case, coalescence would reduce the entropy, without yielding any energetic compensation. We therefore expect that as $\gamma_i \rightarrow 0$ a micro-emulsion will form at the interface, where the smallest droplets which still exhibit IF will be the thermodynamically stable ones, since the larger the droplet, the larger is the entropy loss. Moreover, using surface energy cost consideration, tuning the temperature from above to below T_{mix} should change the shapes of the emulsion's droplets from a spherical shape, which has a minimal surface area, at $\gamma_i > 0$ to an elongated shape with a larger surface area, at $\gamma_i = 0$. We are currently exploring these emulsions by calorimetry and microscopy methods.

The $c = 1.1$ mM curve in Fig. 5 reveals a very large T -range of existence for the IF effect, reaching a maximal value of $\Delta T_i^{\text{max}} = T_i^{\text{max}} - T_b \approx 10^\circ\text{C}$, much larger than the $\sim 1.2^\circ\text{C}$ observed for SF of C16 at the free surface of the melt.⁵ Of course, as $c \rightarrow 0$, T_i decreases, and so does the existence range, $\Delta T_i = T_i - T_b$, as we discuss below. Measurements on water/ C_n /CTAB ($n = 13$ – 16)²¹ and on water/ C_n /STAB ($n = 14, 16$), show that as the chain length n of the alkane decreases below that of the alkyl-TAB's, m , both T_b and T_i^{max} decrease with increasing difference $\delta n = m - n$. However, T_b decreases faster, in agreement with measurements on mixed monolayers of CTAB/ C_n ($n = 11$ – 16) at the air : water interface. This results in an increase in ΔT_i^{max} with δn . This, in turn, allows the vanishing of γ_i to appear at increasingly lower surfactant concentrations c as the length difference between surfactant and alkane, δn , increases. Indeed, preliminary measurements on the water/C14/STAB show that the $\gamma_i(T) = 0$ region appears already at $c = 0.12$ mM, well below, and thus most probably unrelated to, the cmc or the solubility limit, which will be discussed below.

The STAB concentration dependence. The measured variation of T_i with STAB concentration is plotted in Fig. 6 (points). The cmc of STAB in water is also marked. We observed that at $c > \text{cmc}$, a constant value of T_i is found. This point is further discussed below in the context of the phase diagram. Here we just note that this indicates that the areal coverage, Γ , of the solution : C16 interface by the surfactant is saturated at a constant value independent of c . Unfortunately, our measurements, still in progress, do not allow at this stage a confident determination of the absolute coverage Γ , *e.g.* through the Gibbs adsorption rule $\Gamma = -[d\gamma_i/d(\ln(c))]/RT$. However, in the water/C14/CTAB system, the IF effect is induced even by a ten-fold lower Γ_{CTAB} than the ~ 5 molecules nm $^{-2}$ found in SF monolayers at the free surface of the melt, which is practically the same as that in the solid bulk alkane. It is therefore reasonable to assume that the incorporation of C16 molecules into the monolayer of the STAB's stearyl chains, which protrude into the alkane phase, reduces the

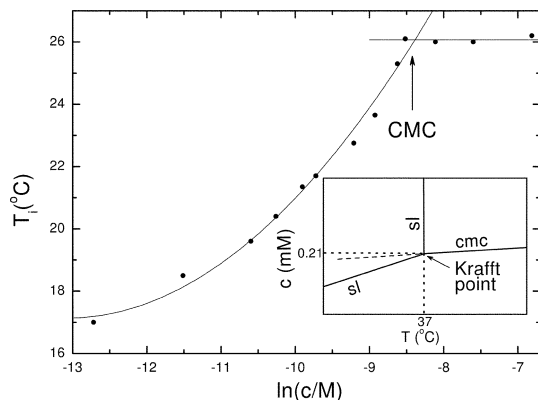


Fig. 6 The measured (points) variation of the IF onset temperature T_i with the molar concentration of STAB. Note the sharp change at the CMC to a constant T_i , due to the saturated, constant interface coverage with STAB. The solid lines are phenomenological linear (above CMC) and parabolic (below CMC) fits to the data. The inset is a scheme of the phase diagram topology near the Krafft temperature. The solubility limit line is marked by sl and the dash line is the metastable continuation of the cmc line below the Krafft temperature.

system's free energy. This creates an interesting new situation, where the interaction parameter between the two types of chains is attractive (negative), driving towards mixing, rather than the repulsive (positive) interaction parameter, driving towards phase separation, for different-length chains at the free surface of alkane mixtures, as discussed above. Since the surface coverage by the surfactant does not change significantly at the transition²¹ the mixing entropy change upon IF is expected to be very small.

As observed in Fig. 6, T_i does not follow the linear dependence on $\ln(c)$, found for the water/C14/CTAB system.²¹ Rather, a phenomenological fit by a polynomial reveals a $T_i \propto [\ln(c)]^2$ dependence, shown by the solid line in the figure. Within the regular solution model, this would indicate a non-zero enthalpy for our system, while that in the water/C14/CTAB should be negligible. We can therefore invoke the theory discussed above for the free surface of mixtures, neglecting the mixing entropy, which changes only marginally in the transition. Equating the chemical potential of the hexadecane in the crystalline (c) and liquid (l) interfacial phases yields for the dependence of T_i on the STAB concentration, an equation equivalent to eqn. (3):

$$T_i = T_{i,0}[1 - \lambda k_B(\phi_1^s)^2/\Delta S] \quad (4)$$

where $\lambda = \omega^j/k_B T$, ω^j is the interaction parameter between the STAB's tail and the C16 molecule in the IF monolayer, and ϕ_1^s is the STAB concentration in the liquid surface phase. ϕ_1^s is obtainable in principle from Gibbs rule, if the c -variation of the absolute γ_i is known accurately. ΔS is the entropy loss upon freezing of C16, and $T_{i,0}$ is the IF temperature of the pure water:C16 interface, even if unobservable due to preemption by bulk freezing. By analogy with the water/C14/CTAB system, we expect that $\phi_1^s \sim \Gamma$ is approximately linear in $\ln(c)$ ²¹. Eqn. (4) then yields a parabolic dependence of T_i on $\ln(c)$, as indeed observed in Fig. 6 for $c < \text{cmc}$. Unfortunately, a fit of eqn. (4) to the measured points is not possible since the absolute ϕ_1^s are not known, as mentioned above.

Equilibrium or metastable? The question of thermodynamic equilibrium in these measurements deserves some consideration. An accurately measured (c, T) phase diagram is not available for STAB in water, to the best of our knowledge. However, a qualitative scheme near the Krafft point is shown in the inset of Fig. 6. The dash line is the (almost T -independent) metastable cmc line, which is the continuation of the equilibrium cmc line below the Krafft point. For STAB in water, this line is always close to the $\text{cmc}(T_K) \approx 0.21 \text{ mM}$,³⁵ where, $T_K = 37^\circ \text{C}$ is the Krafft temperature.³⁶ Above T_K , increasing c past the cmc drives the excess molecules to aggregate in micelles, leaving the bulk concentration, and thus the interface coverage by the surfactant, Γ , constant at the cmc value.³⁷ Below T_K this description still holds, except that now the excess bulk molecules aggregate as a precipitating solid. However, the constancy of the excess surface coverage Γ , and, therefore, the

invariance of $\gamma_i(T)$, upon increasing c above the sl-line are still maintained. It is important to note that all $\gamma_i(T)$ scans in this study are carried out at $T < T_K$. Consequently, we expect the saturation of Γ , and the concomitant onset of the invariance of the $\gamma_i(T)$ curves with increasing c , to be at the sl-line. Even though the position of the sl-line in our system is not known, it is expected to lie considerably lower in c than the cmc(T_K) ≈ 0.21 mM since the sl-line is temperature dependent, as shown in the inset to Fig. 6, and our T_i 's are at least 10 °C below the Krafft point. Nevertheless, as Fig. 6 clearly shows, the onset of the $\gamma_i(T)$ invariance occurs at the cmc. It seems therefore that for concentrations below 0.21 mM down to the (unknown) sl-line, the $\gamma_i(T)$ scans are carried out, at least partly, on a metastable STAB solution. This occurs since the high kinetic barrier against crystal nucleation from the solution of alkyl-TAB surfactants prevents precipitation of the excess molecules upon crossing the sl-line, yielding a metastable, supersaturated solution, the behaviour of which mimics that of a solution above T_K . In particular, it exhibits a crossing of the metastable cmc line upon increasing c , with a consequent onset at this c of the invariance of the $\gamma_i(T)$ scans. This is indeed observed in Fig. 6.

Alkane length dependence. First results on the dependence of the effects discussed above on the alkane length, n , are shown in Fig. 7, for a STAB concentration of 0.15 mM, close to the cmc. The temperature at which the interfacial tension vanishes, T_{mix} , is also shown. Its value for C13 could not be measured due to material purity problems. As can be observed, both T_i and T_b decrease with n . However, the faster decrease of T_b causes $\Delta T(n) = T_i - T_b$ to grow with decreasing n . Since data for $n < 13$ is unavailable, it is not clear whether T_i remains constant with decreasing n , as the values for $n = 13$ and 14 seem to indicate. This, however is not likely. At the other end of the n -range

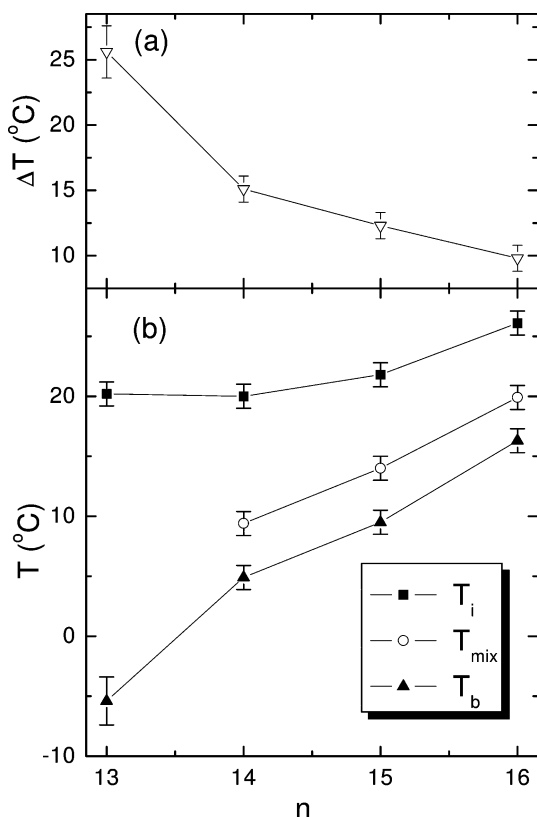


Fig. 7 (a) The temperature difference between the bulk and interface freezing temperatures as a function of the alkane length. (b) The measured (points) variation of the bulk and interface freezing temperatures for various alkane lengths n , for a STAB concentration of 0.15 mM. T_{mix} is also shown.

shown in the figure, T_i and T_b approach each other, so that ΔT is expected to vanish at some n , yet to be determined. This general trend is in agreement with recent measurements by one of us (C.D.B) on CTAB-induced surface freezing of alkane monolayers at the free surface of water.³⁹ For CTAB-induced *interfacial* freezing at the water–alkane interface, C16 (which has a chain length equal to that of CTAB) does not show IF. However, at a 0.6 mM CTAB concentration, C13, C14 and C15 do show IF, with existence ranges of $\Delta T = 13, 5, 3$ °C, respectively.²¹ The trend in $\Delta T(\Delta n = n - 16)$ for CTAB is similar to $\Delta T(\Delta n = n - 18)$ for STAB, albeit the latter is of a larger absolute magnitude. Clearly, measurements over a more extended n range are called for to establish the n -dependence of T_i and T_{mix} (T_b is available in the literature)⁴⁰ before the construction of a theory, even at the thermodynamic level, can be attempted.

Concluding remarks

The results presented here, and, in particular, the rather tentative and approximate calculation of T_i in the previous section, while somewhat preliminary and available for a few systems only at this stage, do provide a glimpse into an intriguing new interfacial phenomenon. A considerably larger body of experimental data, both as a function of the alkane and the surfactant length are required to determine the behaviour of the IF effect for the water/C n /alkyl-TAB system, and the physics underlying this behaviour. These measurements are now in progress. Moreover, X-ray reflectivity, and, if feasible, grazing incidence diffraction measurements on the liquid and frozen interface are required to determine the structure of the IF monolayer in the interface-normal and interface-parallel directions. Such X-ray measurements are extremely demanding, as demonstrated by the liquid–liquid interface measurements of Schlossman and coworkers²⁰ due to two factors. First, there is the need to diffract through a condensed phase (the upper alkane phase) which greatly increases the scattered background. Second, the extremely low γ_i values of these systems, result in large capillary-wave-induced interfacial roughnesses. These, in turn, reduce the reflected and diffracted signals, thereby restricting severely the measurable angular range, and, consequently, the achievable resolution. Nevertheless, even these limited-range measurements may be worthwhile, and are being planned.

Acknowledgements

We thank Henning Kraack and Zvi Sapir (Bar-Ilan) for important discussions and assistance with the measurements.

References

- 1 (a) J. G. Dash, *Contemp. Phys.*, 1989, **30**, 89; (b) R. Lipowsky, *J. Appl. Phys.*, 1984, **55**, 2485; (c) G. An and M. Schick, *Phys. Rev. B*, 1988, **37**, 7534.
- 2 (a) J. W. M. Frenken and J. F. van der Veen, *Phys. Rev. Lett.*, 1985, **54**, 134; (b) H. Dosch, T. Höfer, J. Peisl and R. L. Johnson, *Europhys. Lett.*, 1991, **15**, 527; (c) D. M. Zhu and J. G. Dash, *Phys. Rev. Lett.*, 1986, **57**, 2959; (d) M. Elbaum and M. Schick, *Phys. Rev. Lett.*, 1991, **66**, 1713; (e) S. Chandavarkar, R. M. Geertman and W. H. de Jeu, *Phys. Rev. Lett.*, 1992, **69**, 2384.
- 3 (a) J. C. Earnshaw and C. J. Hughes, *Phys. Rev. A*, 1992, **46**, R4494; (b) X. Z. Wu, E. B. Sirota, S. K. Sinha, B. M. Ocko and M. Deutsch, *Phys. Rev. Lett.*, 1993, **70**, 958.
- 4 (a) B. M. Ocko, A. Braslau, P. S. Pershan, J. Als-Nielsen and M. Deutsch, *Phys. Rev. Lett.*, 1986, **57**, 94; (b) J. Als-Nielsen, F. Christensen and P. S. Pershan, *Phys. Rev. Lett.*, 1982, **48**, 1107; (c) P. S. Pershan and J. Als-Nielsen, *Phys. Rev. Lett.*, 1984, **52**, 759; (d) G. J. Kellogg, P. S. Pershan, E. H. Kawamoto, W. Foster, M. Deutsch and B. M. Ocko, *Phys. Rev. E*, 1995, **51**, 4709.
- 5 B. M. Ocko, X. Z. Wu, E. B. Sirota, S. K. Sinha, O. Gang and M. Deutsch, *Phys. Rev. E*, 1997, **55**, 3164.
- 6 O. Gang, *Surface Ordering in Chain Molecules*, PhD Thesis, Bar-Ilan University, 1999, unpublished.
- 7 O. Gang, X. Z. Wu, B. M. Ocko, E. B. Sirota and M. Deutsch, *Phys. Rev. E*, 1998, **58**, 6086.
- 8 O. Gang, B. M. Ocko, X. Z. Wu, E. B. Sirota and M. Deutsch, *Phys. Rev. Lett.*, 1998, **80**, 1264.
- 9 O. Gang, B. M. Ocko, X. Z. Wu, E. B. Sirota and M. Deutsch, *Phys. Rev. Lett.*, 1999, **82**, 588.
- 10 (a) T. K. Xia and U. Landman, *Phys. Rev. B*, 1993, **48**, 11313; (b) J. G. Harris, *J. Phys. Chem.*, 1992, **96**, 5077; (c) F. A. M. Lermakers and M. A. Cohen Stuart, *Phys. Rev. Lett.*, 1996, **76**, 82; (d) G. A. Sefer, G. Du, P. B. Miranda and Y. R. Shen, *Chem. Phys. Lett.*, 1995, **235**, 347.

- 11 (a) A. Weinstein and S. A. Safran, *Phys. Rev. E*, 1996, **53**, R45; (b) A. ten Bosch, *J. Chem. Phys.*, 1998, **108**, 2228; (c) A. ten Bosch, *Phys. Rev. E*, 2001, **63**, 61808.
- 12 (a) P. Smith P, R. M. Lynden-Bell, J. C. Earnshaw and W. Smith, *Mol. Phys.*, 1999, **96**, 249; (b) H. Z. Li and T. Yamamoto, *J. Phys. Soc. Jpn.*, 2002, **71**, 1083; (c) T. Shimizu and T. Yamamoto, *J. Chem. Phys.*, 2000, **113**, 3359.
- 13 (a) A. V. Tkachenko and Y. Rabin, *Phys. Rev. Lett.*, 1996, **76**, 2527; (b) A. V. Tkachenko and Y. Rabin, *Phys. Rev. Lett.*, 1997, **79**, 532; (c) Y. Rabin, *Phys. Rev. E.*, 1998, **55**, 778.
- 14 A. J. Colussi, M. R. Hoffmann and Y. Tang, *Langmuir*, 2000, **16**, 5213.
- 15 E. B. Sirota, X. Z. Wu, B. M. Ocko and M. Deutsch, *Phys. Rev. Lett.*, 1997, **79**, 531.
- 16 (a) N. Maeda and V. V. Yaminsky, *Phys. Rev. Lett.*, 2000, **84**, 698; (b) H. Gang, J. Patel, X. Z. Wu, M. Deutsch, O. Gang, B. M. Ocko and E. B. Sirota, *Europhys. Lett.*, 1998, **43**, 314.
- 17 (a) C. Merkl, T. Pfohl and H. Riegler, *Phys. Rev. Lett.*, 1997, **79**, 4625; (b) N. Maeda, N. M. Kohonen and H. K. Christenson, *Phys. Rev. E*, 2000, **61**, 7239; (c) H. Schollmeyer, B. Struth and H. Riegler, *Langmuir*, 2003, **19**, 5042; (d) A. Holzwarth, S. Leporatti and H. Riegler, *Europhys. Lett.*, 2000, **52**, 653; (e) Y. Yamamoto, H. Ohara, K. Kajikawa, H. Ishii, N. Ueno, K. Seki and Y. Ouchi, *Chem. Phys. Lett.*, 1999, **304**, 231.
- 18 (a) M. Aratono, T. Takiue, N. Ikeda, A. Nakamura and K. Motomura, *J. Phys. Chem.*, 1992, **96**, 9422; (b) M. Aratono, T. Takiue, N. Ikeda, A. Nakamura and K. Motomura, *J. Phys. Chem.*, 1993, **97**, 5141.
- 19 (a) J. Gliniski, G. Chavapeyer, J. K. Platten and C. De Saedeleer, *J. Colloid Interface Sci.*, 1993, **158**, 382; (b) M. Salajan, J. Gliniski, G. Chavapeyer, J. K. Platten and C. De Saedeleer, *J. Colloid Interface Sci.*, 1994, **164**, 387.
- 20 (a) A. M. Tikhonov, S. V. Pingali and M. L. Schlossman, *J. Chem. Phys.*, in press; (b) M. L. Schlossman and A. M. Tikhonov, in *Mesoscale Phenomena in Fluid Systems*, ed. F. Case and P. Alexandridis, ACS Symposium Series 861, OUP, 2003, p. 81; (c) A. M. Tikhonov and M. L. Schlossman, *J. Phys. Chem. B*, 2003, **107**, 3344.
- 21 Q. Lei and C. D. Bain, *Phys. Rev. Lett.*, 2004, **94**, 176103.
- 22 (a) E. Sloutskin, X. Z. Wu, T. B. Peterson, O. Gang, B. M. Ocko, E. B. Sirota and M. Deutsch, *Phys. Rev. E*, 2003, **68**, 31605–31606; (b) E. Sloutskin, E. B. Sirota, O. Gang, X. Z. Wu, B. M. Ocko and M. Deutsch, *Eur. Phys. J. E*, 2004, **13**, 109.
- 23 X. Z. Wu, B. M. Ocko, E. B. Sirota, S. K. Sinha, M. Deutsch, G. H. Cao and M. W. Kim, *Science*, 1993, **261**, 1018.
- 24 E. Sloutskin, O. Gang, H. Kraack, B. M. Ocko and M. Deutsch, *Phys. Rev. Lett.*, 2002, **89**, 65501.
- 25 E. Sloutskin, H. Kraack, O. Gang, B. M. Ocko, E. B. Sirota and M. Deutsch, *J. Chem. Phys.*, 2003, **118**, 10729.
- 26 (a) J. H. Hildebrand and R. L. Scott, *The Solubility of Nonelectrolytes*, Reinhold, New York, 1950; (b) E. A. Guggenheim, *Mixtures*, OUP, Oxford, 1952; (c) R. Defay, I. Prigogine, A. Bellemans and D. H. Everett, *Surface Tension and Adsorption* Wiley, NY, 1966.
- 27 X. Z. Wu, B. M. Ocko, H. Tang, E. B. Sirota, S. K. Sinha and M. Deutsch, *Phys. Rev. Lett.*, 1995, **75**, 1332.
- 28 R. R. Matheson Jr. and P. Smith, *Polymer*, 1985, **26**, 288.
- 29 G. A. Sefler, Q. Du, P. B. Miranda and Y. R. Shen, *Chem. Phys. Lett.*, 1995, **235**, 347.
- 30 M. M. Knock, G. R. Bell, E. K. Hill, H. J. Turner and C. D. Bain, *J. Phys. Chem. B*, 2003, **107**, 10801.
- 31 (a) D. Turnbull and R. L. Cormia, *J. Chem. Phys.*, 1961, **34**, 3, 820; (b) K. F. Kelton, *Solid State Phys.*, 1991, **45**, 75.
- 32 H. Kraack, E. B. Sirota and M. Deutsch, *J. Chem. Phys.*, 2000, **112**, 6873, and references therein.
- 33 (a) E. B. Sirota and A. B. Herhold, *Science*, 1999, **283**, 529; (b) A. B. Herhold, H. E. King and E. B. Sirota, *J. Chem. Phys.*, 2002, **116**, 9036.
- 34 J. Frenkel, *Kinetic Theory of Liquids*, Clarendon, Oxford, 1946.
- 35 (a) A cmc = 0.31 mM at $T = 34\text{ }^{\circ}\text{C}$ is reported by J. R. Lu, E. A. Simister, R. K. Thomas and J. Penfold, *J. Phys. Chem.*, 1993, **97**, 6024; (b) Jaeger *et al.*,³⁶ however, report a lower value of cmc = 0.28 mM at a higher temperature, $T = 65\text{ }^{\circ}\text{C}$.; (c) J. F. Paddy, *J. Phys. Chem.*, 1967, **71**, 3488, reports yet another value: cmc = 0.15 mM. This, however, was measured at $T = 25\text{ }^{\circ}\text{C}$, well below T_K and may not represent an equilibrium value. In view of this uncertainty we adopted a value of cmc = 0.21 mM extrapolated from CrTAB ($n = 10\text{--}16$) measurements quoted in J. Israelachvili, *Intermolecular and Surface Forces*, 2nd Edn., Academic, London, 1992.
- 36 D. A. Jaeger, G. Li, W. Subotkowski and K. T. Carron, *Langmuir*, 1997, **13**, 5563.
- 37 (a) K. Shinoda and P. Becher, *Principles of Solution and Solubility*, Dekker, New York, 1974; (b) T. Lyklema, *Fundamentals of Interface and Colloid Science*, Academic, London, 1991, vol. 1: *Fundamentals*.
- 38 M. L. Schlossman, *Curr. Opin. Coll. Int. Sci.*, 2002, **7**, 235.
- 39 C. D. Bain, Q.F. Lei and K. Wilkinson, unpublished.
- 40 D. M. Small, *Physical Chemistry of Lipids*, Plenum, New York, 1986.